Understanding the Balance between Ionic and Dispersion Interactions in Aqueous Micellar Media

J. L. DelaCruz and G. J. Blanchard*

Michigan State University, Department of Chemistry, East Lansing, Michigan 48824-1322

Received: January 21, 2003; In Final Form: April 9, 2003

We have studied the interaction of selected rhodamine alkyl esters with cationic, anionic, and neutral micelles to elucidate the balance between ionic and dispersion forces operative in these systems using steady-state and time-resolved optical spectroscopies. The strongest intermolecular interactions with the cationic probes are seen in anionic SDS micelles, where ionic and dispersion interactions are expected to both operate as attractive forces. Weaker interactions are seen between the probes and cationic CTAB micelles, owing to the repulsive ionic interactions counteracting dispersion interactions. Interactions of the probes with the neutral Thesit micelle are intermediate between results for SDS and CTAB, and we observe the general trend that as the rhodamine aliphatic ester chain is lengthened, the interaction of the chromophore with the micelle is stabilized to a greater extent.

Introduction

Amphiphilic systems are important to a number of chemical processes ranging from the existence of lipid bilayers to the use of detergents in industrial and home applications. The single feature of amphiphiles that gives rise to such broad utility is their ability to coexist with and function as an interface between polar and nonpolar phases. This ability is determined by a balance between ionic and dipolar interactions with polar media and dispersion interactions with nonpolar media. Micelles are a subset of amphiphilic systems that manifest transient self-assembly behavior in certain concentration regimes, and this family of solution-phase aggregates has been studied extensively.

Micelles have attracted significant attention because of their ability to function as encapsulating and biomimetic systems. Among the properties of micelles that have been investigated are the effects of amphiphile concentration on size, shape, and permeability, and time-domain optical spectroscopy has emerged as a useful tool for such studies. Many studies of micelles have focused on associating a probe molecule with the micellar environment and correlating the observed dynamics of the probe molecule with that of the micelle as a function of pressure, viscosity, and probe solubility.[1−19]

Despite the widely held understanding that the formation and existence of micelles represents a balance between dispersion and ionic or dipolar intermolecular interactions, a detailed understanding of this balance remains to be articulated. The approach taken to understanding the behavior of micellar systems has been to use an optical probe that exhibits limited solubility in both the micelle and the aqueous phase, with the dynamical response of the system modeled in the context of the simultaneous observation of the same chromophore in multiple environments. The rationale for interpreting dynamical data within this framework has been the observation of biexponential induced orientational anisotropy decays, with the assumption that the chromophore in each environment is characterized by a single-exponential anisotropy decay. Except for systems designed to force the chromophore into one environment or the other, chromophores will establish a dynamic equilibrium between the two phases and a significant issue in understanding such data is the time scale of dynamic exchange relative to the time scale of the reorientation measurements.

We expect that the environment of a micelle will vary in a regular manner as a function of distance from the center of the micelle, going from a relatively dense aliphatic medium near the center to a relatively diffuse region known as either the Stern layer in charged micelles, or as the Palisade layer in neutral micelles,[20−22] where the headgroups, counterions, and solvent molecules coexist. Several groups have performed studies using chromophores that were not water soluble, but were soluble in the aliphatic portions of the micelle, and recovered the result that these chromophores partitioned between different regions within the micelle.[3,4,7,8,12,19,23] We are interested in exploring the structural factors that can influence the balance of forces that allows such partitioning to occur. To elucidate these factors, we have performed rotational diffusion measurements using four rhodamine derivatives with varying aliphatic ester chain lengths. These are tetramethylrhodamine-methyl ester (R1), tetramethylrhodamine-ethyl ester (R2), tetraethylrhodamine-hexyl ester (R6), and tetraethylrhodamine-octadecyl ester (R18), (Figure 1) in three different aqueous micellar environments: cetyltrimethylammonium-bromide (CTAB), sodium dodecyl sulfate (SDS), and poly(ethylene glycol) 400 dodecyl ether (Thesit) (Figure 1). The rhodamines are a family of robust chromophores that have found wide use as optical probes. These cationic dyes are water soluble and are thus good candidates for studies of micellar systems. Our data point to the expected partitioning between aqueous and micellar phases, with the details of the partitioning depending sensitively on the identity of the micelle headgroups and the probe aliphatic chain length. We find that, for Thesit, the rhodamine hexyl ester partitions into the micellar phase with anomalous efficiency, suggesting the importance of geometric issues in determining probe−micelle interactions.

Experimental Section

Pump−Probe Laser System. The picosecond pump−probe laser spectrometer used to acquire reorientation data on the

* Author to whom correspondence should be addressed. E-mail: blanchard@chemistry.msu.edu.

10.1021/jp034163w CCC: $25.00
Published on Web 06/25/2003

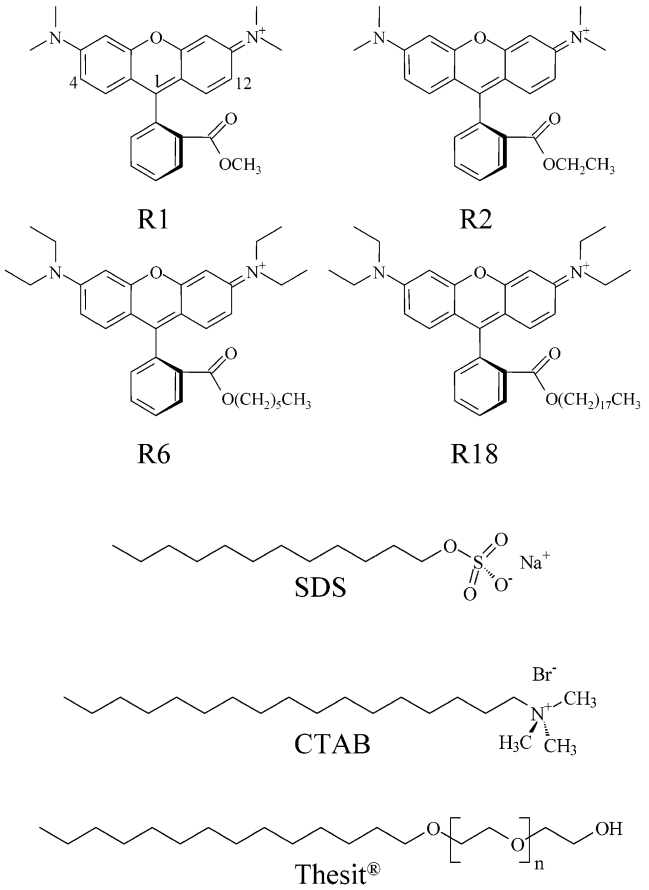

Figure 1. Rhodamines and surfactants used in this study. Top row, left to right: tetramethylrhodamine methyl ester (R1), tetramethylrhodamine ethyl ester (R2). Second row, left to right: tetraethylrhodamine hexyl ester (R6), tetraethylrhodamine octadecyl ester (R18). Third row: sodium dodecyl sulfate (SDS). Fourth row: cetyltrimethylammonium bromide (CTAB). Bottom row: poly(ethylene glycol) 400 dodecyl ether (Thesit).

chromophores in water has been described in detail previously,[24] and we present only a brief synopsis of its operation here. A mode-locked CW Nd:YAG laser (Coherent Antares 76-S) produces 30 W of average power (1064 nm, 100 ps pulses, 76 MHz repetition rate). The output of this laser is frequency-doubled to produce ~3 W of average power at 532 nm, with the same pulse duration and repetition rate. The second harmonic light is used to excite two cavity-dumped dye lasers (Coherent 702-3) synchronously, with the output of both lasers being ~110 mW average power at 8 MHz repetition rate, producing ~7 ps fwhm autocorrelation traces using a three-plate birefringent filter. The pump dye laser was operated using Pyromethine 567 dye (Exciton) at 556 nm, and the probe laser was operated with Rhodamine 6G dye (Kodak) at 580 nm. The pump and probe wavelengths were chosen to access the $S_1 \leftarrow S_0$ transition of each chromophore to detect the stimulated emission from each probe. The probe laser polarization was set alternately to 0° and 90° relative to the pump laser polarization for individual time-domain scans of parallel ($I_{\parallel}(t)$) and perpendicular ($I_{\perp}(t)$) polarization used in constructing the orientational anisotropy function. The time resolution of this system, ~10 ps, is determined by the cross-correlation of the pump and probe laser pulses. Detection of the transient signals was accomplished using a radio- and audio-frequency triple-modulation scheme, with synchronous demodulation detection.[25−27] The reorientation time constants we report here are the average of 6 individual determinations, each comprised of the average of 10−12 sets of $I_{\parallel}(t)$ and $I_{\perp}(t)$ scans.

Time-Correlated Single-Photon Counting Measurements. Rotational diffusion measurements of the probes in micellar systems were made using a spectrometer that has been described previously,[24] and we provide a synopsis of its essential features here. The source laser is a mode-locked CW Nd:YAG laser (Quantronix 416) producing 7 W average power at 1064 nm with 100 ps pulses at 80 MHz repetition rate. The second harmonic of the output of this laser (532 nm, ~700 mW) is used to excite a synchronously pumped, cavity-dumped dye laser (Coherent 702-2) operating with Pyromethine 567 dye (Exciton) at 556 nm. The output of this laser is typically 100 mW average power with a 4 MHz repetition rate and 5 ps pulses. Detection of the transient fluorescence signals was accomplished using a microchannel plate photomultiplier tube (Hamamatsu R3809U), with fluorescence light collection through a reflecting microscope objective and wavelength selection with a subtractive double monochromator (American Holographics DB-10). The electronics used for the signal processing are a Tennelec 455 quad constant fraction discriminator and a Tennelec 864 time-to-amplitude converter and biased amplifier. The reference channel was detected and delayed using an in-house built fiber optic delay line. Signals are processed using a multichannel analyzer (PCA Multiport II) and sent to a PC for acquisition. For this system, the instrument response function is typically 30−35 ps fwhm.

Steady-Sate Spectroscopy. The steady-state absorption spectra of the chromophores used here were recorded with 1 nm resolution using a Cary model 300 UV−visible spectrophotometer. The spontaneous emission spectra for the same solutions were obtained with 1 nm resolution using a SPEX Fluorlog-3 spectrometer.

Chemicals and Sample Handling. The probe molecules tetramethylrhodamine-methyl ester perchlorate (R1), tetramethylrhodamine-ethyl ester perchlorate (R2), tetraethylrhodamine-hexyl ester perchlorate (R6), and tetraethylrhodamine-octadecyl ester chloride (R18) (Figure 1) were obtained from Molecular Probes Inc. and used as received. Distilled, deionized water was available in-house. The chromophore concentration of all solutions used for laser measurements was 10 μM. Measurements of R18 solutions in neat water were hampered by bleaching of the solution. This effect was mitigated by replacement with fresh solution on at least a daily basis, or as warranted. All pump−probe measurements were taken using a flowcell with a 1 mm path length, and TCSPC data were acquired using a fluorescence cuvette with a 1 cm path length. Solution temperatures were maintained at 298 ± 0.5 K (Neslab EX100-DD).

The surfactants sodium dodecyl sulfate (SDS), cetyltrimethylammonium bromide (CTAB), and poly(ethylene glycol) 400 dodecyl ether (Thesit) (Figure 1) were obtained from Sigma-Aldrich, Inc., checked for fluorescent impurities, and used as received.

Results and Discussion

We are interested in using rhodamine alkyl esters as probes of micellar behavior. Previous studies of rhodamines have provided a substantial understanding of their optical properties and the relationship(s) between chromophore structure and intermolecular interactions.[28−32] Using this knowledge, we consider how to interrogate the balance of forces that give rise to micellar structures in aqueous amphiphile solutions. We have selected a series of rhodamine aliphatic esters with the idea that the ester aliphatic tails will interact preferentially with the

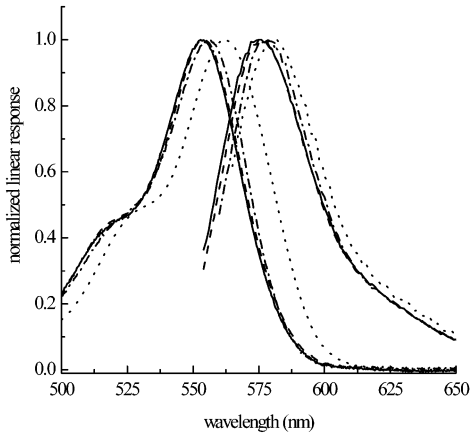

Figure 2. Normalized absorption and emission spectra of the rhodamine esters in water. R1 = solid line, R2 = dashed line, R6 = dotted line, and R18 = dash−dot line.

interior of the micelle and the cationic rhodamine chromophore will interact primarily with the micelle headgroups. For anionic SDS micelles, intuition suggests that attractive ionic interactions between chromophore and micelle headgroup will dominate and for cationic micelles, intuition suggests that repulsive ionic interactions will play the primary role. For these systems, the extent to which the chromophores partition into the micelles depends sensitively on the chromophore aliphatic chain length. For neutral Thesit micelles it is not clear *a priori* whether attractive or repulsive polar interactions will dominate. To evaluate whether these expectations are realistic, we have examined the steady-state spectroscopy and reorientation behavior of the rhodamine esters in water and aqueous micellar media.

Linear Optical Response. The normalized absorption and emission spectra of the chromophores studied here are shown in Figure 2. With the exception of R6, the absorption and emission spectra of all the chromophores are not influenced to a significant extent by increasing the length of the ester chain. R6 exhibits a slight red-shift of ∼7 nm in its absorption and emission spectra. Drexhage has studied the structure−spectroscopy relationships for rhodamines,[33] and his work has shown that the *o*-benzoate ring at the 1-position of these chromophores (Figure 1) is essentially decoupled from the three-ring chromophore system, precluding a direct electronic effect from being responsible for the spectral shift we observe for R6. It is well established that substituents at the 4 and 12 positions (Figure 1) do influence the spectral profiles of the rhodamines, and interactions between the ester aliphatic chain and the protons at the 4 and/or 12 positions could, in principle, account for our findings. If such a sterically mediated interaction does account for our spectral data, it remains unclear why the same spectral shifts are not seen for R18, and this is a matter that bears further investigation. Semiempirical calculations (HyperChem v. 6.0) predict no anomalous red-shift for long chain rhodamine esters. Thin-layer chromatography (TLC) experiments show no unresolved impurities in our raw material and no other indications of anomalies were apparent in our solution preparation procedures.

Time-Resolved Spectroscopy. Experimental time-domain data ($I_{||}(t)$ and $I_{\perp}(t)$) are combined according to eq 1 to produce the induced orientational anisotropy function, $R(t)$.

$$R(t) = \frac{I_{||}(t) - I_{\perp}(t)}{I_{||}(t) + 2I_{\perp}(t)} \tag{1}$$

TABLE 1: Reorientation Times and Zero-time Anisotropies for Rhodamine Chromophores in Aqueous and Micellar Environments

		water[a]	SDS[b]	CTAB[b]	Thesit[b]
R1	$R_1(0)$	0.25 ± 0.03	0.05 ± 0.02	0.29 ± 0.01	0.32 ± 0.04
	τ_1 (ps)	132 ± 15	243 ± 118	152 ± 13	160 ± 6
	$R_2(0)$		0.27 ± 0.03	0.02 ± 0.01	0.04 ± 0.01
	τ_2 (ps)		1037 ± 48	1405 ± 399	1558 ± 298
R2	$R_1(0)$	0.22 ± 0.03	0.05 ± 0.02	0.34 ± 0.03	0.30 ± 0.01
	τ_1(ps)	129 ± 15	311 ± 111	166 ± 3	151 ± 9
	$R_2(0)$		0.26 ± 0.02	0.01 ± 0.01	0.04 ± 0.02
	τ_2(ps)		1024 ± 120	1869 ± 494	1558 ± 207
R6	$R_1(0)$	0.27 ± 0.04	0.03 ± 0.01	0.23 ± 0.02	0.13 ± 0.04
	τ_1(ps)	172 ± 32	97 ± 14	200 ± 31	87 ± 34
	$R_2(0)$		0.28 ± 0.01	0.08 ± 0.02	0.23 ± 0.02
	τ_2(ps)		1142 ± 32	1481 ± 543	1361 ± 59
R18	$R_1(0)$	0.22 ± 0.03	0.02 ± 0.02	0.17 ± 0.02	0.23 ± 0.01
	τ_1(ps)	145 ± 21	190 ± 88	149 ± 18	200 ± 21
	$R_2(0)$		0.25 ± 0.01	0.14 ± 0.01	0.08 ± 0.02
	τ_2(ps)		1101 ± 36	1275 ± 92	2189 ± 676

[a] The data are the best fit results of the data to the function $R(t) = R(0)\exp(-t/\tau_{or})$. Time constants are in ps and the uncertainties are standard deviations ($\pm 1\sigma$) for at least five determinations of each quantity. [b] The values reported are the best fit results of the data to the function $R(t) = R_1(0)\exp(-t/\tau_1) + R_2(0)\exp(-t/\tau_2)$. Time constants are in ps and the uncertainties are standard deviations ($\pm 1\sigma$) for at least five determinations of each quantity.

The functionality of the $R(t)$ decay provides important information on the dynamics of the chromophores. All of the rhodamine esters exhibit single-exponential anisotropy decays in water and biexponential decays in micellar environments. We used pump−probe measurement for chromophore reorientation in water because of its time resolution and sensitivity to fast decay components. TCSPC measurements were used for micellar systems to allow acquisition of data over a longer time window than is accessible using pump−probe methods. Our previous work has shown that the $S_1 \leftarrow S_0$ transitions we access are oriented along the rhodamine chromophore long axis. In water, the rhodamine esters behave as prolate rotors. For all data, the reported zero-time anisotropies are derived from the regression of the data for times greater than 15 ps after excitation, and the uncertainties reported for each quantity are 95% confidence intervals for six or more individual determinations. We report the zero-time anisotropies and orientational relaxation time constants for the rhodamine esters in aqueous and micellar environments in Table 1.

The data we present in this paper for the reorientation of the rhodamine esters in water (Figure 3) are predicted reasonably well by the Debye−Stokes−Einstein (DSE) model in the stick limit.[34]

$$\tau_{OR} = \frac{\eta V f}{k_B T S} \tag{2}$$

where τ_{OR} is the orientational relaxation time, V is the solute hydrodynamic volume, f is a frictional coefficient ($f = 1$ in the stick limit), k_B is the Boltzmann constant, T is the temperature in K, and S is a shape factor to account for deviations from a spherical shape for the reorienting moiety. We note that R18 reorients on a time scale that is faster than the other rhodamine esters and is indeed faster than that predicted by the modified DSE model.[34−36] We understand this behavior on the basis of the ester alkyl chain length interacting with the chromophore in such a manner as to screen the ionic charge of the chromophore, thus promoting more "slip"-like behavior[35] of the chromophore. Even though the hydrodynamic volume of the chromophore increases (R1 = 360 Å^3, R2 = 377 Å^3, R6 =

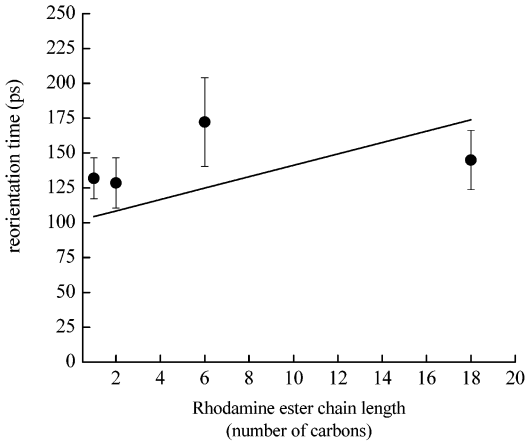

Figure 3. Time-resolved reorientation data for rhodamines in the aqueous phase as a function of calculated hydrodynamic volume. Solid circles are experimental data points, and the solid line is the reorientation time calculated using the modified Debye−Stokes−Einstein equation in the stick limit. For R1 and R2, the shape factor *S* is calculated to be 0.84 on the basis of molecular geometry, and for R6 and R18, *S* is taken to be 1 because of the shape uncertainty introduced by the presence of the longer aliphatic chains.

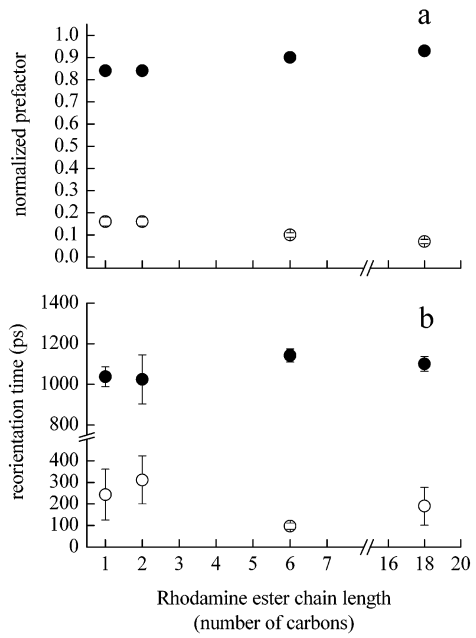

Figure 4. Data for rhodamine aliphatic esters in aqueous SDS micelle solution. Biexponential anisotropy decay functions produced (a) normalized prefactors for the contribution of the fast (○) and slow (●) components of the anisotropy decays. (b) Reorientation time constants plotted as a function of increasing ester chain length.

513 Å^3, R18 = 717 Å^3),[37,38] the frictional interaction decreases in such a way as to compensate for the change in probe volume. We note that the counterion for R18 (Cl^-) is different than that for the other rhodamine esters (ClO_4^-). Earlier work has shown that the effect of counterion on the reorientation of molecules of this size is either negligible, or very slight at most,[39] and cannot account for our findings.

The reorientation data presented here for the rhodamine esters in micellar environments are different from those of the reorientation of these same chromophores in water, with biexponential anisotropy decays being seen for reorientation in micellar solutions (Figures 4−6). The simplest interpretation of the data is that the chromophore reorients either in the water portion of the environment or within the micelles. Examination

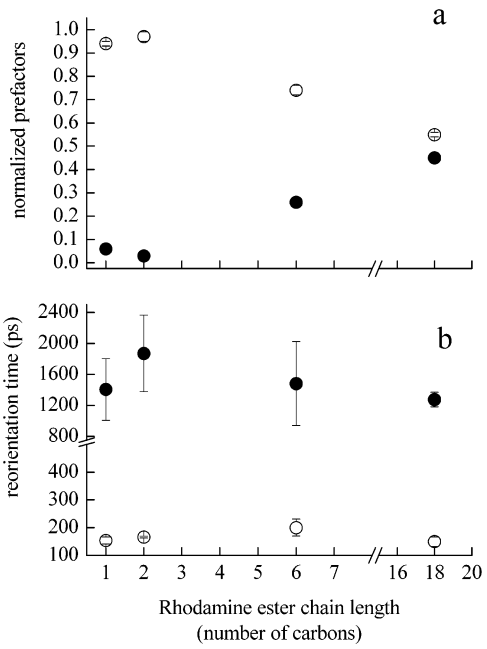

Figure 5. Data for rhodamine aliphatic esters in aqueous CTAB micelle solution. Biexponential anisotropy decay functions produced (a) normalized prefactors for the contribution of the fast (○) and slow (●) components of the anisotropy decays. (b) Reorientation time constants plotted as a function of increasing ester chain length.

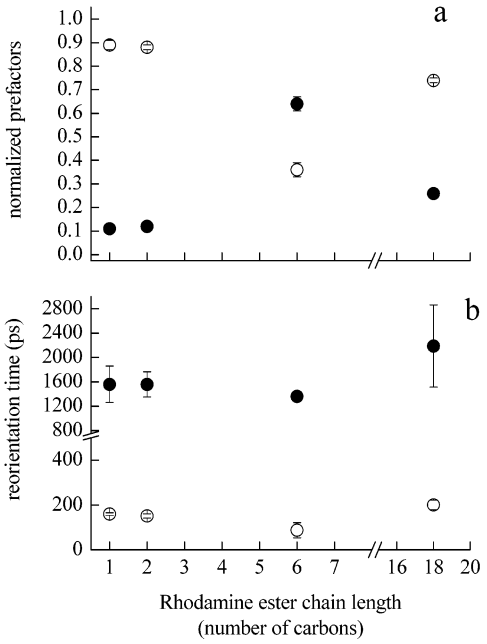

Figure 6. Data for rhodamine aliphatic esters in aqueous Thesit micelle solution. Biexponential anisotropy decay functions produced (a) normalized prefactors for the contribution of the fast (○) and slow (●) components of the anisotropy decays. (b) Reorientation time constants plotted as a function of increasing ester chain length.

of the experimental time constants shows this not to be the case, because the fast reorientation time components do not match those for reorientation in water. There are, in principle, at least two other ways to interpret a biexponential $R(t)$ decay in these systems. The first way is to consider that we observe hindered motion of a chromophore bound to the micelle, i.e. motion in a single, restricted environment. In this model, the anisotropy function exponential prefactors are determined by the spectroscopic properties of the chromophore and are predictable.[40−45] Of most significance is that, for all of these systems, we would

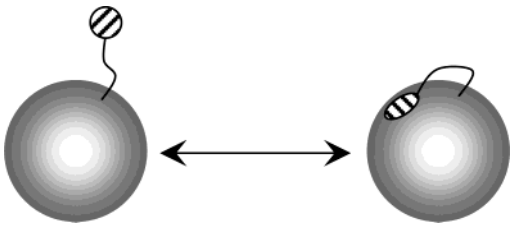

Figure 7. Schematic representation of equilibrium between loosely bound and tightly bound rhodamine alkyl ester chromophores in micelles. This cartoon does not imply any specific geometry for the interaction(s) between the chromophore and the micelle.

expect similar prefactors for all reorientation measurements if hindered rotation accounted for our findings. We do not find this to be the case experimentally (Figures 4−6). Our data show that the exponential prefactors in the biexponential anisotropy decay depend sensitively on both the rhodamine alkyl tail length and on the identity of the micelle. While we have found the hindered rotor model to be useful for interpreting molecular motion in micellar media in previous studies, this model is not likely to be physically realistic for the rhodamine methyl and ethyl esters. In addition, the predictions of the hindered rotor model cannot account for the exponential prefactors we observe in a manner consistent with the structures of the rhodamines. For these reasons, we offer the following interpretation of our data. We assert that our data can be understood in terms of the chromophore being bound to the micelle and interacting with it strongly, or being associated loosely with the micelle, and an equilibrium exists between these two conditions (Figure 7). In this picture, the chromophore aliphatic tail interacts with the inner aliphatic region of the micelle, and the length of the aliphatic tail mediates the chromophore proximity to the micelle and thus its freedom of motion. The distribution of the chromophore between relatively polar and relatively nonpolar environments can be estimated through the normalized preexponential factors (R_1* and R_2* for short- and long-time component preexponential factors) as shown in eq 3.

$$R_1^* = \frac{R_1}{R_1 + R_2}$$

$$R_2^* = \frac{R_2}{R_1 + R_2} \tag{3}$$

This treatment assumes that the transition moment angle characteristic of a given chromophore does not depend sensitively on its local environment and, for the systems we consider here, this is likely to be an excellent approximation.[46]

The experimental data for the reorientation of the chromophores in anionic SDS micellar solution (33 mM, 4× cmc) are shown in Figure 4 and Table 1. These data show that $R(t)$ decays biexponentially for all chromophores. For all of the rhodamine esters, we recover the same time constants, to within the experimental uncertainty. The average time constants for the two decays, 210 ± 82 ps and 1076 ± 59 ps, are measurably different than the average reorientation time seen for water (144 ± 21 ps), despite the fact that the *bulk* viscosity of the SDS solution is essentially the same as that of water. We note that there are experimental reports that suggest a high microviscosity for SDS and CTAB micellar systems,[47] and such high microviscosities are consistent with the slow components of the anisotropy decays we measure. More information is required, however, to evaluate the relationship between micelle microviscosity and reorientation times owing to the undetermined average residence time of the chromophore in the micelle. Our observation of a two-component anisotropy decay suggests an interaction of the rhodamines with the micelle, which we would expect on the basis of simple ionic association arguments. The overall motion of SDS micelles is predicted to be on the several nanosecond time scale,[14,15,45] and the ∼1100 ps time constant we recover appears to be too fast to account for micelle motion. The chromophores do not yield time constants consistent with being bound rigidly in the micelle, or free to rotate in an aqueous environment.

The reorientation dynamics of the rhodamine esters in cationic CTAB micellar solution (3.0 mM, 3× cmc) are shown in Figure 5. For these systems, there seems to be no clear dependence of the reorientation time (Table 1) on increasing ester chain length. As with reorientation in SDS micelles, the recovered time constants do not correspond to independent motion of the chromophores within the micelle (too fast), or the motion of the micelle itself (too slow).

For the reorientation of the rhodamine esters in the neutral Thesit system (1.0 mM, 10× cmc), it is not clear how the balance of forces will operate, i.e., whether polar and dispersion interactions will act in a cooperative or opposing manner. Inspection of the individual time constants for the rhodamines reveal that the interaction between the chromophores and the micellar system is anomalous for the hexyl ester. There is a decrease in the time constants measured for R6 and this behavior is unique to the R6/Thesit system. This trend is also seen in the chromophore partitioning data (Figure 6). Starting with the ethyl ester, there is an increase in the chromophore partitioning into the micelle to the point where the chromophore is interacting with the micelle core more strongly than with the headgroup. This trend is reversed for R18, counter to any predictions that can be made solely on the basis of energetic trends.

We assert that the same fundamental physics is operative in all of these systems; fast motion is indicative of the cationic rhodamine chromophore headgroup existing in a region somewhat separated from, but tethered to the micelle, and that the slow motion is reflective of the rhodamine chromophore associated more tightly with the micelle. Thus the normalized anisotropy prefactors R_1* and R_2* are proportional to the concentrations of the loosely bound (C_l) and tightly bound species (C_t), respectively. If there exists a dynamic equilibrium between these association conditions, we can use the concentration ratios to obtain the equilibrium constant, which is related to the free energy of interaction between the micelle and chromophore.

$$\mathrm{C_l} \overset{K_{eq}}{\rightleftharpoons} \mathrm{C_t}$$

$$K_{eq} = \frac{[\mathrm{C_t}]}{[\mathrm{C_l}]} \approx \frac{R_2^*}{R_1^*}$$

$$\Delta G = -RT \ln K_{eq} \tag{4}$$

The free energy we extract from these data can be decomposed into polar and dispersion contributions.

$$\Delta G = \Delta G_{polar} + \Delta G_{dispersion} \tag{5}$$

We can estimate the $\Delta G_{dispersion}$ as follows. For highly ordered aliphatic chains, such as alkanethiol monolayers on gold, the energy of interaction between chains is taken to be ∼ −1.25 kJ/mol-CH_2.[42,43] We believe this value to be too high for micellar systems owing to the significantly lower extent of aliphatic chain

TABLE 2: Various Thermodynamic Properties of Rhodamine Chromophores in SDS and CTAB Micellar Environments

	K_{eq}	ΔG_{total}	ΔG_{disp}	ΔG_{polar}
		SDS		
R1	5.40	−4.21	−0.5	−3.71
R2	5.20	−4.11	−1.0	−3.11
R6	9.33	−5.57	−3.0	−2.57
R18	12.5	−6.30	−9.0	+2.70
		CTAB		
R1	0.07	+6.63	−0.5	+7.13
R2	0.03	+8.67	−1.0	+9.67
R6	0.35	+2.61	−3.0	+5.61
R18	0.82	+0.50	−9.0	+9.50
		Thesit		
R1	0.12	+5.18	−0.5	+5.68
R2	0.13	+4.98	−1.0	+5.98
R6	1.77	−1.41	−3.0	+1.59
R18	0.35	+2.59	−9.0	+11.59

[a] All ΔG values are in units of kJ/mol. Values for ΔG_{total} are calculated from eq 3. Values for ΔG_{polar} are calculated from eq 4.

ordering in these systems. We *estimate* the strength of interaction to be −0.5 kJ/mol-CH_2 unit, and calculate the ionic contribution to the interaction energy as a function of rhodamine alkyl ester chain length. It can be argued that this estimate is either too high or too low, but it is important to keep in mind that the actual energy of interaction is confined to a relatively small range, between no interactions (0 kJ/mol) and those of a crystalline-like system (−1.25 kJ/mol). In addition, we note that, even with a different estimate of the value of the average aliphatic interaction energy, the trends revealed by this interpretation of the data remain unchanged. We present the results calculated from eqs 4 and 5 for SDS and CTAB micelles in Table 2. The results show that the chromophore interaction with the micelle headgroup region is significant, and the dependence of the data on rhodamine alkyl ester chain length reveals the important role of the electric double layer around the perimeter of the (ionic) micelles.

When the data on chromophore distribution are examined, a clear picture emerges of increasing chromophore interaction with CTAB as a function of increasing ester chain length (Figure 5a). Much like the SDS micelles, the interaction is primarily with the headgroup region for the methyl and ethyl esters, and then increases substantially for the hexyl and octadecyl esters. This effect is dominated by the increase in dispersion interactions between the micelle aliphatic region and the chromophore ester alkyl chains. The effects of polar/ionic interactions are compensated substantially by the presence of the electric double layer at the micelle perimeter. From the results for polar interaction energies reported in Table 2, it can be seen that the strength of polar interactions remains relatively constant and repulsive with increasing probe alkyl chain. Specifically, we recover a polar interaction energy term for probe−SDS systems that becomes increasingly unfavorable with increasing probe alkyl chain length, and a polar interaction remains approximately constant for interactions between CTAB and the rhodamine probes. While intuition would suggest strongly attractive ionic interactions between the probe and SDS, with the overall interaction increasing in strength as the probe alkyl ester length increased, this is not what is seen experimentally. We find approximately constant total interaction energy for the probes with SDS, with ionic interactions becoming increasingly unfavorable with increasing alkyl chain length. For these systems, the dominant ionic interactions are between the probe cationic moiety and the electric double layer at the perimeter of the micelle. For SDS, the counterions are Na^+ and H^+ and these ions will interact repulsively with the cationic rhodamine. As the probe alkyl ester chain length is increased, the probe is drawn more efficiently into the micelle and repulsive interactions between the micelle electric double layer and the probe headgroup become more pronounced. For CTAB, the opposite result is obtained. The ionic interactions between the rhodamine probe and the CTAB counterions (Br^-) in the proximity of the micelle headgroups remain essentially constant (∼8.5 kJ/mol) as a function of rhodamine alkyl ester chain length. For CTAB, the ionic interactions are essentially constant and appear to be mediated by the presence of the counterions at the micelle surface. We note that, despite the importance of polar interactions being between the micelle counterions and the cationic probe, the magnitude of the interactions for both systems are similar, and modest.

For Thesit, the overall driving forces for association are intermediate between those seen for SDS and CTAB (Table 2). This is an expected result. The data point to similar interactions for R1 and R2, likely because of the small relative contributions of the dispersion forces to the probe−micelle interaction. With increasing rhodamine alkyl chain length, we find more favorable interactions for R6 than for R18. It is likely that, for this system, interactions between the polar micelle mantle and the chromophore are optimized for R6 for steric reasons. It is not clear why there is a relatively large, unfavorable polar interaction term for R18, but one possibility is that the chromophore is in closer proximity to the nonpolar micellar core for this system. Further experimentation will be required to elucidate this issue.

Conclusions

We have studied the steady-state spectroscopy and reorientation dynamics of selected rhodamine esters in water and in the aqueous micellar systems, SDS, CTAB, and Thesit. The charges of the rhodamines and the lengths of the ester chains dictate that there is an interaction with each of these micellar systems and we have used this interaction to probe the balance of forces operating between micelles and amphiphilic probes. The reorientation dynamics of the chromophores reveal two environments for the chromophores interacting with the micelles: a tightly bound environment and one where the probe interacts more weakly with the micelle, characterized by greater motional freedom. For the ionic micelles, the role of the electric double layer formed by counterions is substantial in mediating either repulsive or attractive ionic interactions. For Thesit, the absence of an ionic double layer and the presence of substantial disorder in the mantle region gives rise to behavior that is qualitatively consistent with that seen in the ionic micelles, but differing in detail. Because of the ionic compensation effect we observe, dispersion interactions assume substantial importance in determining the dynamics of micellar media.

Acknowledgment. We are grateful to the National Science Foundation for its support of this work through Grant 0090864.

References and Notes

(1) Jarzeba, W.; Walker, G. C.; Johnson, A. E.; Kahlow, M. A.; Barbara, P. F. *J. Phys. Chem.* **1988**, *92*, 7039.

(2) Visser, A. J. W. G.; Vos, K.; van Hoek, A.; Santema, J. S. *J. Phys. Chem.* **1988**, *92*, 759.

(3) Marcus, A. H.; Dichun, N. A.; Fayer, M. D. *J. Phys. Chem.* **1992**, *96*, 8930.

(4) Quitevis, E. L.; Marcus, A. H.; Fayer, M. D. *J. Phys. Chem.* **1993**, *97*, 5762.

(5) Cho, C. H.; Chung, M.; Lee, J.; Nguyen, T.; Singh, S.; Vedamuthu, M.; Yao, S.; Zhu, J.-B.; Robinson, G. W. *J. Phys. Chem.* **1995**, *99*, 7806.
(6) Streletzky, K.; Phillies, G. D. J. *Langmuir* **1995**, *11*, 42.
(7) Nandi, N.; Bagchi, B. *J. Phys. Chem.* **1996**, *100*, 13914.
(8) Maiti, N. C.; Krishna, M. M. G.; Britto, P. J.; Periasamy, N. *J. Phys. Chem. B* **1997**, *101*, 11051.
(9) Matzinger, S.; Hussey, D. H.; Fayer, M. D. *J. Phys. Chem. B* **1998**, *102*, 7216.
(10) Riter, R. E.; Willard, D. M.; Levinger, N. E. *J. Phys. Chem. B* **1998**, *102*, 2705.
(11) Willard, D. M.; Riter, R. E.; Levinger, N. E. *J. Am. Chem. Soc.* **1998**, *120*, 4151.
(12) Pal, S. K.; Mandal, D.; Sukul, D.; Bhattacharyya, K. *Chem. Phys. Lett.* **1999**, *312*, 178.
(13) Bhattacharyya, K.; Bagchi, B. *J. Phys. Chem. A* **2000**, *104*, 10603.
(14) Pal, S. K.; Sukul, D.; Mandal, D.; Sen, S.; Bhattacharyya, K. *Chem. Phys. Lett.* **2000**, *327*, 91.
(15) Cang, H.; Brace, D. D.; Fayer, M. D. *J. Phys. Chem. B* **2001**, *105*, 10007.
(16) Hara, K.; Kuwabara, H.; Kajimoto, O. *J. Phys. Chem. A* **2001**, *105*, 7174.
(17) Sen, S.; Sukul, D.; Dutta, P.; Bhattacharyya, K. *J. Phys. Chem. A* **2001**, *105*, 7495.
(18) Mandal, D.; Sen, S.; Bhattacharyya, K.; Tahara, T. *Chem. Phys. Lett.* **2002**, *359*, 77.
(19) Dutt, G. B. *J. Phys. Chem. B* **2002**, *106*, 7398.
(20) Berr, S. S.; Caponetti, E.; Johnson, J. S.; Jones, R. R. M.; Magid, L. J. *J. Phys. Chem.* **1986**, *90*, 5766.
(21) Berr, S. S.; Coleman, M. J.; Jones, R. R. M.; Johnson, J. S. J. *J. Phys. Chem.* **1986**, *90*, 6492.
(22) Berr, S. S. *J. Phys. Chem.* **1987**, *91*, 4760.
(23) Kawato, S.; Kinosita, K., Jr.; Ikegami, A. *Biochemistry* **1978**, *17*, 5026.
(24) Dewitt, L.; Blanchard, G. J.; Legoff, E.; Benz, M. E.; Liao, J. H.; Kanatzidis, M. G. *J. Am. Chem. Soc.* **1993**, *115*, 12158.
(25) Blanchard, G. J.; Wirth, M. J. *Anal. Chem.* **1986**, *58*, 532.
(26) Andor, L.; Lorincz, A.; Siemion, J.; Smith, D. D.; Rice, S. A. *Rev. Sci. Instrum.* **1984**, *55*, 64.
(27) Bado, P.; Wilson, S. B.; Wilson, K. R. *Rev. Sci. Instrum.* **1982**, *53*, 706.
(28) Ferguson, J.; Mau, A. W. H. *Chem. Phys. Lett.* **1972**, *17*, 543.
(29) Rosenthal, I.; Peretz, P.; Muszkat, K. A. *J. Phys. Chem.* **1979**, *83*, 350.
(30) Pevenage, D.; Van der Auweraer, M.; De Schryver, F. C. *Langmuir* **1999**, *15*, 8465.
(31) Kohn, F.; Hofkens, J.; De Schryver, F. C. *Chem Phys. Lett.* **2000**, *321*, 372.
(32) Ghanadzadeh, A.; Zanjanchi, M. A. *Spectrochim. Acta, Part A* **2001**, *57*, 1865.
(33) Drexhage, K. H. In *Dye Lasers*, 2nd ed.; Schaefer, F. P., Ed.; Springer: Berlin, 1977; p 144.
(34) Debye, P. *Polar Molecules*; Chemical Catalog Co.: New York, 1929.
(35) Hu, C.-M.; Zwanzig, R. *J. Chem. Phys.* **1974**, *60*, 4354.
(36) Perrin, F. *J. Phys. Radium* **1934**, *5*, 497.
(37) Youngren, G. K.; Acrivos, A. *J. Chem. Phys.* **1975**, *63*, 3846.
(38) Fleming, G. R.; Knight, A. E. W.; Morris, J. M.; Robbins, R. J.; Robinson, G. W. *Chem. Phys. Lett.* **1977**, *51*, 399.
(39) Blanchard, G. J. *J. Phys. Chem.* **1991**, *95*, 5293.
(40) Horne, J. C.; Blanchard, G. J. *J. Am. Chem. Soc.* **1996**, *118*, 12788.
(41) Horne, J. C.; Blanchard, G. J. *J. Am. Chem. Soc.* **1998**, *120*, 6336.
(42) Horne, J. C.; Blanchard, G. J. *J. Am. Chem. Soc.* **1999**, *121*, 4427.
(43) Horne, J. C.; Blanchard, G. J.; Legoff, E. *J. Am. Chem. Soc.* **1995**, *117*, 9551.
(44) Horne, J. C.; Huang, Y.; Liu, G. Y.; Blanchard, G. J. *J. Am. Chem. Soc.* **1999**, *121*, 4419.
(45) Kelepouris, L.; Blanchard, G. J. *J. Phys. Chem. B* **2002**, *106*, 6600.
(46) Kelepouris, L.; Krysinski, P.; Blanchard, G. J. *J. Phys. Chem. B* **2003**, *107*, 4100.
(47) Pal, S. K.; Datta, A.; Mandal, D.; Bhattacharyya, K. *Chem. Phys. Lett.* **1998**, *288*, 793.